SIMULATION AND ANALYSIS OF GaAs/AlGaAs MULTIPLE QUANTUM WELL ELECTRO-ABSORPTION MODULATOR

THESIS REPORT

Submitted in partial fulfillment of the requirements for the award of the Degree of Master of Technology in Electronics and Communication Engineering with specialization in Communication Systems by the A P J Abdul Kalam Technological University

by

SRUTHI SUNIL MATHEWS

TKM21ECCS12

DEPARTMENT OF ELECTRONICS AND COMMUNICATION ENGINEERING

TKM COLLEGE OF ENGINEERING

KOLLAM 691005

MAY 2023

SIMULATION AND ANALYSIS OF GaAs/AlGaAs MULTIPLE QUANTUM WELL ELECTRO-ABSORPTION MODULATOR

THESIS REPORT

Submitted in partial fulfillment of the requirements for the award of the Degree of Master of Technology in Electronics and Communication Engineering with specialization in Communication Systems by the A P J Abdul Kalam Technological University

by

SRUTHI SUNIL MATHEWS

TKM21ECCS12

DEPARTMENT OF ELECTRONICS AND COMMUNICATION ENGINEERING

TKM COLLEGE OF ENGINEERING

KOLLAM 691005

MAY 2023

DEPARTMENT OF ELECTRONICS & COMMUNICATION ENGINEERING

TKM COLLEGE OF ENGINEERING

KOLLAM 691005

CERTIFICATE

Certified that this thesis report entitled **"SIMULATION AND ANALYSIS OF GaAs/AlGaAs MULTIPLE QUANTUM WELL ELECTRO-ABSORPTION MODULATOR"** is a bonafide report of the work done by **SRUTHI SUNIL MATHEWS** (Reg.No.TKM21ECCS12) in partial fulfillment of the requirement for the award of the Degree of Master of Technology in Electronics and Communication Engineering with specialization in Communication Systems by the A P J Abdul Kalam Technological University during the year 2022-2023.

Coordinator & Guide	**External Guide**	**HoD**
Dr. NISHANTH N	**Dr. SOORAJ R**	**Prof. SHABEER S**
Professor	Associate Professor	Head, Dept. of ECE
Dept. of ECE, TKMCE	Dept. of Avionics, IIST	TKMCE

Acknowledgement

First and foremost, I thank the **ALMIGHTY GOD** for endowing me with immense blessings that helped me in each step of progress toward the successful completion of this project presentation.

I express my sincere thanks to **Prof. SHABEER S**, HOD, Department of Electronics and Communication Engineering, for the support and encouragement during the course of this project presentation.

I take this opportunity to express my sincere gratitude and profound thanks to our Project Coordinator and guide, **Dr. NISHANTH N**, Professor, Department of Electronics and Communication Engineering, for his advice, great support, and unfailing supervision throughout the course of project preparation and presentation.

I express my sincere thanks to **Dr. SOORAJ R**, Associate Professor, Department of Avionics, IIST for his valuable guidance and suggestions throughout the course of preparation and for providing critical inputs in the project preparation and presentation.

I also express my heartfelt thanks to all the faculty members of the Department of Electronics and Communication Engineering, I would like to thank my parents, family members, and all friends for their valuable support during the course of my project preparation and presentation.

SRUTHI SUNIL MATHEWS

TKM21ECCS12

ABSTRACT

With an increase in internet traffic, both long distance fiber networks and short-reach interconnections in data centres demand large-capacity optical transceivers. To achieve the proper transmission distances, symbol rates, and modulation formats in optical transceivers, directly modulated lasers, Electro-Absorption Modulators(EAM), and Mach-Zender Modulators(MZM) are, respectively needed. Because it offers a small footprint, high bandwidth, and low power consumption, the EAM is a crucial component for data centre applications.The Multiple Quantum Well(MQW) based structures has applications in optical modulators and switches. How to make optical transceivers with EAMs smaller and less expensive is a crucial concern.

This work focuses on the simulation of GaAs/AlGaAs MQW EAM and analysis of absorption spectrum with and without the electric field by taking into consideration the different well width of the quantum well. The different mole fractions of $Al_xGa_{1-x}As$ and variation in the number of quantum wells is also taken into consideration for this analysis. Increasing the number of QW shows an increase in absorption coefficients. The operating wavelength is found to be 874.803nm, the wavelength at which the zero field absorption is of a minimum value but applying field causes a higher absorption value. The combination which has less insertion loss is also analysed.

Index Terms—Electro-Absorption Modulator, External Modulation, Tunneling, Absorption.

Contents

Abbrevations

AlGaAs Aluminium Gallium Arsenide

EAM Electro-Absorption Modulator

FKE Franz-Keldysh Effect

GaAs Gallium Arsenide

MQW Multiple Quantum Well

QCSE Quantum Confined Stark Effect

QW Quantum Well

Notations

α	Absorption Coefficient
E_g	Energy gap
x	Mole fraction of $Al_xGa_{1-x}As$
λ_{op}	Operating Wavelength

List of Figures

List of Tables

Chapter 1

Introduction

1.1 Optical Modulation

Optical modulation is a technique for controlling an optical wave or encoding information on a carrier optical wave. Demodulation is the inverse procedure that restores the encoded information. There are several forms of optical modulation, which may be classified in a variety of ways.

1.1.1 Optical Signal Modulation Techniques

In general, there are two ways for modulating an optical signal. These two techniques are classified as follows:

- Direct Modulation
- Indirect Modulation

1.1.2 Direct Modulation

As the name implies, it is a modulation technique in which the data to be communicated is directly put over a light stream generated by the source. Simply altering the driving current of a light source, i.e; the laser, with the electrical information signal generates a changing optical power signal in this manner. As a result, individual optical modulators are not required for optical signal modulation. The main disadvantage of this modulation approach is related to the carrier duration for spontaneous

and stimulated emission, as well as the photon lifetime of the source.

The laser turns on and off in accordance with the electrical signal or the driving current while conducting direct modulation with the laser transmitter. But in this instance, the laser line width is increased in some manner. This increase in laser line width is referred to as chirp.

1.1.3 External Modulation

External modulation employs independent optical modulators that modify optical signals to alter signal properties. After the light is produced, external modulation is carried out. A dc current is used to power the laser, and modulation is performed independently after that. Here, chirping is reduced. The Electro-Optic Modulation and Electro-Absorption Modulation are examples.

1.1.4 Advantages of External Modulation

The advantages of external modulation are:

- Improved chirp performance
- Low driving voltage
- Much faster in processing
- High bandwidth
- Can be integrated with lasers on a single chip resulting in faster/lower chirp modulation than direct modulation by the laser

1.2 Electro-Absorption Modulator(EAM)

An optical modulator known as an Electro-Absorption Modulator is a semiconductor-based device that can change the intensity of a beam of light by using an external electric voltage. The Franz-Keldysh Effect (FKE), which states that a change in the bandgap energy is produced by the applied electric field, forms the foundation of an

EAM. Modulators with low modulation voltages and compact dimensions are preferred in telecommunications. For this sort of external modulation technology, the EAMs are suitable. Bulk semiconductor materials, materials with many quantum dots, or materials with wells can be used to create these modulators. The majority

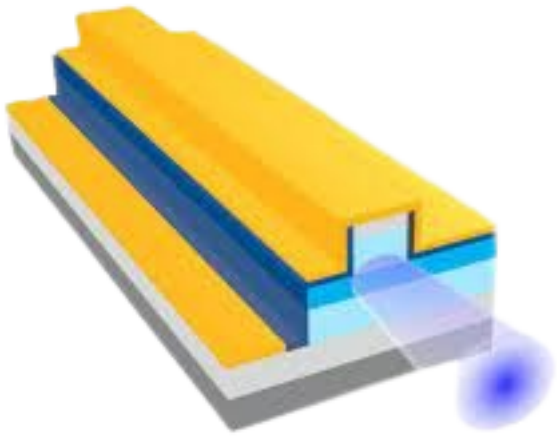

Figure 1.1: Electro-Absorption Modulator

of EAMs are constructed in waveguide form with electrodes to provide an electric field perpendicular to the modulated light beam. In a quantum well structure, the Quantum-Confined Stark Effect (QCSE) is frequently utilized to obtain a high extinction ratio. In comparison to an Electro Optic Modulator(EOM), an EAM may operate at substantially lower voltages(a few volts instead of ten volts or more). Due to their ability to operate at extremely high speeds and achieve modulation bandwidths of tens of gigahertz, these devices are useful for optical fibre communication.

A valuable feature is the ability to merge an EAM and distributed feedback laser diode on a single chip to produce a photonic integrated circuit that acts as a data transmitter. In comparison to direct modulation of the laser diode, higher bandwidth and less chirp may be produced. Interest in the study of self-organized quantum dots has recently increased due to developments in crystal growth. The ability to fabricate quantum dots with improved electro-absorption coefficients makes them interesting for this application since the EAM needs compact size and low modulation voltages.

1.3 Basic Operating Principles of EAM

The practical EAM is semiconductor devices based on FKE, in case of a bulk semiconductor.EAM also known as Quantum Well(QW) Modulator works based on the principle of QCSE. Stark Effect is simply the shift in the absorption spectrum. That is shift in the absorption lines in presence of applied electric field.

1.3.1 Franz-Keldysh Effect(FKE)

The FKE describes how absorbing a photon with energy below the band gap can allow an electron in a valence band to be excited into a conduction band. When the photon energy is below the bandgap, tunnelling permits the electron and hole wave functions to overlap. The Figure 1.2 shows the Tunneling effect.

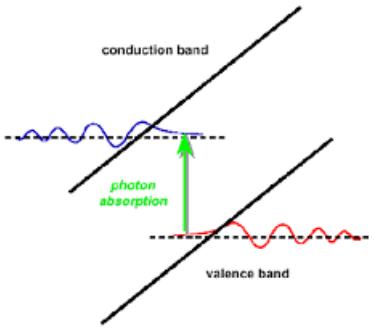

Figure 1.2: Tunneling Effect

1.3.2 Quantum Confined Stark Effect(QCSE)

The QCSE defines the impact of an external electric field on a QW light emission or absorption spectrum. Electrons and holes inside the quantum well are only able to occupy states within a specific range of energy sub-bands in the absence of an external electric field. This lowers the frequency of emission or absorption of light that are allowed. The overlap integral decreases as a result of the external electric field's shifting of electrons and holes to the opposing sides of the well, which also lowers the system's efficiency of recombination. The Figure 1.3 shows the QCSE.

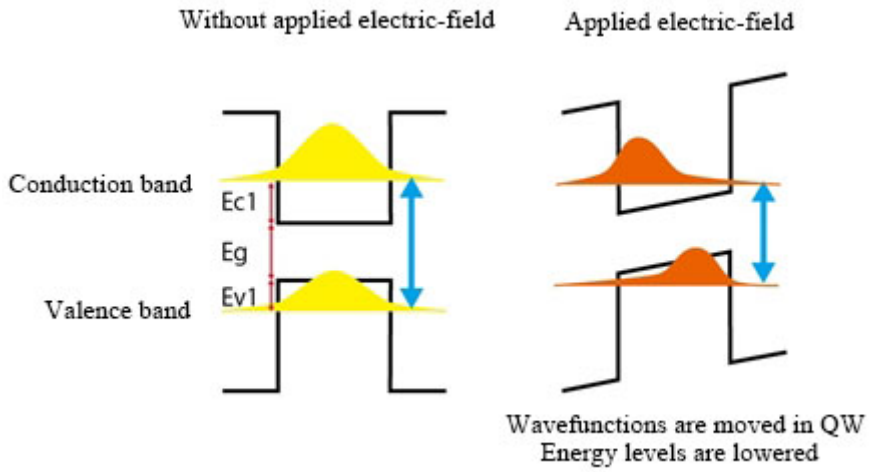

Figure 1.3: QCSE

1.4 Working of Electro-Absorption Modulator

The Electro-Absorption Effect is the change of a material's absorption coefficient (*alpha*) resulting from an external electric field. The intensity of a light beam flowing through the material may be controlled directly using this effect. A Multi-Quantum Well (MQW) structure is made up of alternating small and big bandgap semiconductor layers. The applied electric field alters the energy levels in these structures, causing the absorption edge to move towards lower frequencies or higher wavelengths (QCSE).

When no electric field is applied, light is passed via the modulator. When the electric field is raised, the absorption spectrum moves towards lower frequency/higher wavelength (red shift), and the modulator transforms from transparent to highly absorbing, lowering the intensity of the transmitted light. The intensity of the output light can be calculated using the equation 1.1

$$I_o = I_{in} \times e^{(-\alpha L)} \tag{1.1}$$

where;

- I_o = Intensity of output beam
- I_{in}= Intensity of input beam
- α = Absorption Coefficient

- L = Length of the modulator

1.5 Absorption Coefficient(α)

The absorption coefficient specifies how far a substance can penetrate before absorbing light of a specific wavelength. For various semiconductors, the absorption coefficient varies.

- Depends on:
    1. Wavelength(λ)
    2. Mole Fraction(x)
    3. Length of Modulator(L)
    4. Field Applied(F)

1.6 Insertion Loss(I.L)

The insertion loss is the power loss due to insertion of a device. In order to maximise performance and power efficiency, it should be minimised. The insertion loss of EAM is calculated using equation 1.2. The insertion loss in dB is calculated using equation 1.3. The insertion loss can be as good as 1dB.

$$I.L = 1 - e^{(-\alpha_0 L)} \tag{1.2}$$

$$I.L(dB) = 4.343[1 - e^{(-\alpha_0 L)}] \tag{1.3}$$

1.7 Extinction Ratio(E.R)

The ratio between the optical power at maximum absorption to optical power at minimum absorption. The equation is as shown in equation 1.4

$$E.R(dB) = 4.343[\alpha_{(V)} - \alpha_{(0)}]L \tag{1.4}$$

1.8 Operating Wavelength(λ_{op})

The wavelength at which the zero field absorption is of a minimum value but applying field causes a higher absorption value.

Chapter 2

Literature Review

This section presents an overview of some works and details related to the work done.

Thomas H Wood [1] proposed that since the electro-absorption effect in MQW semiconductor materials is around 50 times greater than that in bulk semiconductors, there is a lot of interest in using MQWs in optical modulators. Small, high-speed devices have been developed that hold promise for optical transmission systems, external modulators, as well as for the encoding and processing parts of optical interconnect and signal processing systems. The use of these modulators, which are constructed using III-V semiconductors, has sparked interest in integrating them with other active opto-electronic components. Although 0.85μm wavelength has traditionally been used by most photonics engineers, there has been significant success recently in adapting this technology for devices that function at around 1.55μm. For fibre optic transmission, 850nm, 1300nm and 1550nm are the three primary wavelengths. Due to the fact that they have the lowest fibre attenuation, these wavelengths are employed in fibre optics. A wave's attenuation rate and length are directly correlated. The longer the wave, the lower the attenuation. These wavelengths are excellent for creating transmission lasers and signal detectors. The paper deals with and reviews the works of the last few years in the field of MQW modulators.

The focus is on devices that operate near the band gap of the constituent semiconductors. It is inferred that the absorption coefficient of the material in the modulator can be manipulated by FKE, QCSE, Excitonic absorption, changes in the fermi level,

and changes of free carrier concentration. Small size and low voltage are desired for a modulator. Capacitance can be reduced by increasing the thickness of the undoped 'i' layer in the p-i-n diode. The speed of the device can be doubled by doubling the thickness of the depletion layer, at a cost of doubling the drive voltage of the device. To increase the maximum achievable change in the absorption coefficient, grow more Quantum well. However this will increase the required voltage.

Chin et.al., [2] proposed that for optical on-off modulators, low insertion loss, high Contrast Ratio (CR), low drive power, and high bandwidth or bit-rate are necessary. Here, based on the QCSE, is a methodical way to improve the overall performance of these modulators. The strategy involves lowering the power-bandwidth ratio to fulfill a specific CR and insertion loss. With a thin buried active layer, this concept combines a large-core multimode passive waveguide.

S.Panda et.al., [3] proposed that the effects of the electric field on the electron sub band energies and wavefunctions in a single QW of $Al_xGa_{1-x}As$ / GaAs/ $Al_xGa_{1-x}As$ can be calculated using an analytical method that accounts for the fluctuation of the effective mass at the barriers. Comparisons are made between the results and prior calculations that took into account the effective mass of GaAs within and outside the well. With the aid of the estimated energies, wavefunctions, and linewidth widening, it is possible to calculate the inter-sub-band optical absorption spectra as well as the shift in the real component of the index of refraction in the well. When different semiconductors are grown one layer at a time utilizing molecular beam epitaxy methods, an energy band offset occurs as a result, which generates the quantum well. The discrete energy levels in a quantum well are created by the charge carriers being quantum-confined. In this work, the Airy function technique is used to determine the Quantum Confined Stark Shift(QCSS) and the mean tunneling lifespan.

P.L. Souza et.al., [4] put forward the idea that the basic equipment for long-distance communication are amplitude modulators. Their research began with the FKE or electro-absorption of bulk material. Attention has been focused on multiple quantum well designs where the QCSE might enhance device performance at high data rates since high-frequency applications required bigger absorption variations with the electric field. This paper clearly shows that the quantum well width cannot be increased further to reduce the applied electric voltage.

T. Hiraki et.al., [5] indicated that with increasing Internet traffic, large-capacity optical transceivers are required for not only long-distance fiber links but also short-reach interconnections in data-centres. In optical transceivers, directly modulated lasers, EAMs, and MZMs are respectively required for appropriate transmission distances, symbol rates, and modulation formats. The EAM is a key component for data centre applications because it provides a small footprint, large bandwidth, and low power consumption. A critical issue is how to reduce the size and cost of optical transceivers containing EAMs.

R. Dingle et.al., [6] indicated that Quantum levels associated with carrier confinement in extremely thin, molecular beam-grown $Al_xGa_{1-x}As/GaAs/Al_xGa_{1-x}As$. As heterostructures result in significant structure in the GaAs optical absorption spectrum. Also indicated that the absorption is negligible in case of mole fraction of $Al_xGa_{1-x}As$ less than 0.2 and there should be a higher bandgap energy for better absorption.

Wight et.al., [7] suggested that a 390 μm wide waveguide modulator has been developed with corresponding insertion loss less than 10% (0.4 dB) and extinction ratio more than 750 (29 dB) with regard to an optical bandwidth and evident that these modulators, when inserted into waveguides. Also suggested that these will be perfectly suitable with micro-electronic circuits and offer novel features and improved capabilities up to and possibly beyond the limiting bandwidths currently anticipated in GaAs high speed electronics. Additionally, these modulators also serve as voltage activated detectors.

L. Ji et.al., [8] proposed that the length of a device has a significant impact on the extinction ratio and insertion loss of EA modulators. And shown that the the suggested modulator's extinction ratio and insertion loss rely heavily on the graphene length of L. The length of 120μm is used to achieve an extinction ratio of 28 dB as well as an insertion loss of 1.28 dB.

Chapter 3

Methodology

The work is done to analyse the QCSE and also to analyse the absorption spectra with and without the application of electric field varying the parameters like well width, mole fraction of the $Al_xGa_{1-x}As$, electric field, number of quantum well used in the MQW Layer(intrinsic layer), etc. The work is done to investigate the operating wavelength also. The insertion loss of respective combinations is also studied.

3.1 Device Structure

The length of the GaAs substrate is taken as 3μm, width as 0.6μm and height as 0.1612μm. The length of the MQW layer region is 3μm and width is 0.6μm. Again below the MQW layers superlattice material of $Al_xGa_{1-x}As$ of 0.53μm height is placed. Then GaAs of 0.3μm of GaAs is placed as the n type bottom. GaAs is taken as the substrate material of height 0.1612μm. And finally at the bottom cathode is placed [9] [10]. The temperature is set as 300K in MQW solver. The simulated model of $Al_xGa_{1-x}As/GaAs$ is shown in Figure 3.1.

The work is done to compare the absorption coefficient of $Al_xGa_{1-x}As/GaAs$ taking into account the different mole fractions of $Al_xGa_{1-x}As$. Here $Al_xGa_{1-x}As$ has higher bandgap than GaAs. The GaAs is considered as the well material and $Al_xGa_{1-x}As$ as the barrier material. The barrier height is taken as 20nm. The parameters like well width, number of QW, mole fraction of The QCSE effect is also analysed. In QCSE the Quantum refers to the QW. The probability of tunneling depends on the width and height of the barrier. As we increase the field, the band

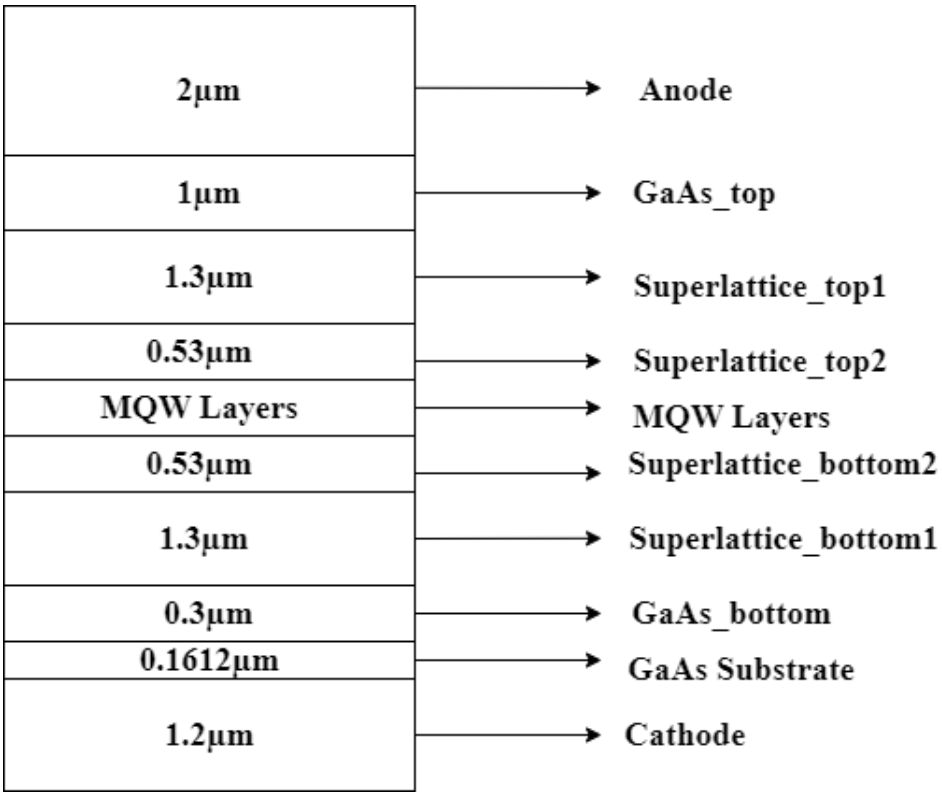

Figure 3.1: Device Structure

diagram will tilt more.

3.2 Software Used

The simulation is done using the software Ansys Lumerical. A software which aids in the design of photonic systems, circuits, and other elements.

3.3 FDE Simulation

First of all, an EAM is designed in FDE simulation and using FDE solver the effective index, group index and confinement factor is found according to different mole fractions of $Al_xGa_{1-x}As$. The refractive index spectra of AlGaAs/GaAs with one and two quantum well is analyzed with varying well width. The output is extracted as a JavaScript Object Notation(JSON) file to be used in next stages.

The FDE Simulated model is as shown in Figure 3.2

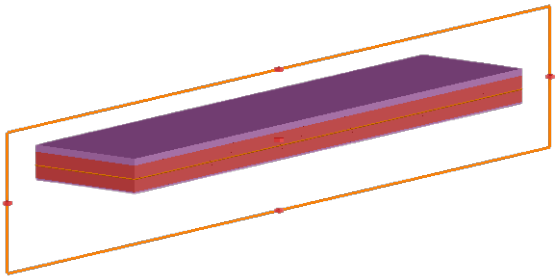

Figure 3.2: FDE Simulated Structure

3.4 MQW Simulation

The JSON file created from FDE solver is uploaded in MQW solver. And using the values from FDE simulated results another EAM is designed in MQW solver. The temperature is set as 300K in MQW solver. Here we have to provide the bandgap energy separately [11] according to the given equation 3.1.

$$Eg = 1.424 + 1.247(x); 0 < x < 0.45 \tag{3.1}$$

where x denotes the mole fraction of $Al_xGa_{1-x}As$. The mole fraction is taken from 0.20 to 0.40 with a difference of 0.02 difference. The same is done for one QW and two QW separately. The MQW simulated model is as shown in Figure 3.3.

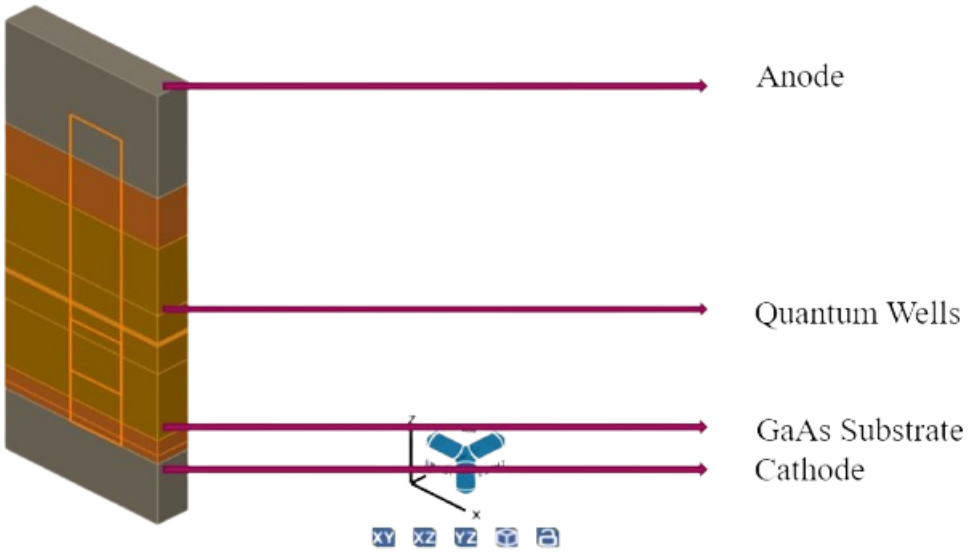

Figure 3.3: MQW Simulated Model

Mole Fraction(x)	Bandgap Energy(E_g)eV
0.10	1.5487
0.12	1.57364
0.14	1.59858
0.16	1.62352
0.18	1.64846
0.20	1.6734
0.22	1.69834
0.24	1.72328
0.26	1.74822
0.28	1.77316
0.30	1.7981
0.32	1.82304
0.34	1.84798
0.366	1.87292
0.38	1.89786
0.40	1.9228

Table 3.1: Bandgap Energy of different mole fractions of $Al_xGa_{1-x}As$

The theoretical formula for finding the absorption coefficient of electron transition is as follows (equation 3.2).

$$\alpha(E) = \frac{4\pi^2 q^2 |e.p_{cv}(0)|^2}{nm_0^2\omega_c}\frac{|\phi(0)|^2}{d}.|\int_{-d/2}^{d/2}\epsilon_e(z)\epsilon_e(z)|^2 g(\epsilon) \tag{3.2}$$

where, "n" is the refractive index of MQW, "ω" is angular frequency of incident light, m_0 the free electron mass, "P_{cv}" Polarization vector of incident light, "q" is the elementary charge, "c" is the velocity of light and "d" is momentum matrix of electron under transition from the valance band to conduction band at zone center. "$\epsilon_e(z)$" and "$\epsilon_h(z)$" is the normalized energy eigen functions of electron and hole respectively. "$\phi(p)$" is the projection of the exciton wave function on the layer plane, and "g(E)" denotes the excitonic absorption coefficient line broadening [12].

3.5 Combinations Simulated

The material composition of $Al_xGaAs_{1-x}As$ was varied from 0.10 to 0.40 in stepss of 0.02. The well width was varied from 5nm to 15nm. The number of quantum wells considered was one and two. And these combinations were simulated using the software Ansys Lumerical.

3.6 Calculation of QCSE

The QCSE is commonly seen in III-V quantum well structures. The device structure is p-i-n type structure. The sides are attached to a metal contact. Aluminium is used for anode and cathode with length 3μm and width 0.6μm. For the p type top region a length of 3μm, width 0.6μm and of height 1μm GaAs is used. Below that the superlattice top of $Al_xGa_{1-x}As$ of height 1.3μm is taken and below that superlattice layer of $Al_xGa_{1-x}As$ of 0.53μm is placed. The QCSE in $Al_xGa_{1-x}As/GaAs$ is analyzed here. The quantum well is formed by making heterojunctions of different bandgaps. The well material is GaAS and the barrier material is $Al_xGa_{1-x}As$.

The length of the GaAs substrate is taken as 3 μm, width as 0.6μm and height as 0.1612μm . The length of the MQW layer region is 3μm and width is 0.6μm. Again below the MQW layers superlattice material of $Al_xGa_{1-x}As$ of 0.53μm height is placed. Then GaAs of 0.3μm of GaAs is placed as the n type bottom. GaAs is taken as the substrate material of height 0.1612μm. And finally at the bottom cathode is placed [9] [10]. The temperature is set as 300K in MQW solver. The simulated model of $Al_xGa_{1-x}As/GaAs$ is shown in Figure 3.3.

Chapter 4

Results and Discussion

4.1 Analysis of QCSE Spectra

The FDE simulation is done using FDE solver in Ansys Lumerical. From which the effective index, group index and confinement factor is calculated. Then the simulation is done for different mole fractions of $Al_xGa_{1-x}As$ using the Charge/MQW solver. The results obtained from FDE simulation of well width of 5nm is shown in Table 4.1 and Table 4.2.

The results obtained from FDE simulation of well width of 9.4nm is given in Table 4.3, Table 4.4. Similarlly the results of well width of 15nm is shown in Table 4.6 and Table 4.5. The other FDE simulation results are shown in Table 4.7.

4.1.1 Effect of Electric Field on Band Diagram

In the Figure 4.1 and Figure 4.2 Ec denotes the conduction band and Ev denotes the valence band. The band diagram of the multiple quantum well without any applied electric field is shown in Figure 4.1. By the application of an electric field, the band diagram gets tilted, it is shown in Figure 4.2. And it allows photon assisted tunneling to conduction band from the valance band. As we increase the field, the tilting increases.

Mole Fraction(x)	Effective Index	Group Index	Confinement Factor	Eg(eV)
0.10	3.51318+0.0181195	4.87873	0.0372872	1.5487
0.12	3.50511+0.0182427i	4.72007	0.0372453	1.57364
0.14	3.50574+0.0182158i	4.6184	0.0417592	1.59858
0.16	3.50672+0.0180469i	4.52814	0.043976	1.62352
0.18	3.50696+0.01789671i	4.45245	0.0450877	1.64846
0.20	3.50699+0.0177848i	4.38861	0.0455631	1.6734
0.22	3.50175+0.0177032i	4.33329	0.0457726	1.69834
0.24	3.50609+0.0176497i	4.28594	0.045927	1.72328
0.26	3.50647+0.0176808i	4.2421	0.0461688	1.74822
0.28	3.50538+0.0175623i	4.204845	0.0465784	1.77316
0.30	3.5024+0.017522i	4.173846	0.0471081	1.7981
0.32	3.4921+0.0174973i	4.151319	0.0476044	1.82304
0.34	3.4861+0.0174694i	4.129786	0.0479672	1.84798
0.36	3.47807+0.0174449i	4.1091	0.0482026	1.87292
0.38	3.47011+0.0174259i	4.08938	0.0483558	1.89786
0.40	3.46219+0.0174123i	4.07064	0.0484651	1.9228

Table 4.1: Effective Index, Group Index, Confinement Factor and Bandgap Energy corresponding to various mole fractions with 1 QW for well width=5nm

Mole Fraction(x)	Effective Index	Group Index	Confinement Factor	Eg(eV)
0.12	3.50451+0.018285i	4.72154	0.0382607	1.57364
0.20	3.50638+0.0178719i	4.39043	0.0478318	1.6734
0.22	3.5066+0.0177839i	4.33545	0.0483498	1.69834
0.24	3.50566+0.0177263i	4.2883	0.049763	1.72328
0.26	3.50553+0.017678i	4.24492	0.0501438	1.74822
0.28	3.50585+0.0176388i	4.20488	0.0506101	1.77316
0.30	3.50291+0.0176148i	4.17303	0.0502208	1.7981
0.32	3.49475+0.0176187i	4.14951	0.0520786	1.82304
0.34	3.48666+0.0176002i	4.12909	0.0518944	1.84798
0.36	3.47866+0.017592i	4.10978	0.0526626	1.87292
0.38	3.47069+0.0175579i	4.09053	0.0532944	1.89786
0.40	3.4628+0.0175407i	4.07213	0.053817	1.9228

Table 4.2: Effective Index, Group Index, Confinement Factor and Bandgap Energy corresponding to various mole fractions with 2 QW for well width=5nm

Mole Fraction(x)	Effective Index	Group Index	Confinement Factor	Eg(eV)
0.20	3.50727+0.01786051i	4.38868	0.0508375	1.6734
0.22	3.506555+0.0177837i	4.33471	0.0513666	1.69834
0.24	3.5064+0.0177254i	4.28647	0.0.0518202	1.72328
0.26	3.50614+0.0176808i	4.24355	0.0523488	1.74822
0.28	3.50281+0.017602i	4.17426	0.0538714	1.77316
0.30	3.50281+0.0176021i	4.17426	0.0538714	1.7981
0.32	3.49464+0.0175819i	4.15174	0.0546812	1.82304
0.34	3.50281+0.0176021i	4.17426	0.0538714	1.84798
0.36	3.50281+0.017602i	4.17426	0.0538714	1.87292
0.38	3.47061+0.0175209i	4.09017	0.0563725	1.89786
0.40	3.50281+0.017602i	4.17426	0.0538714	1.9228

Table 4.3: Effective Index, Group Index, Confinement Factor and Bandgap Energy corresponding to various mole fractions with 1 QW for well width=9.4nm

Mole Fraction(x)	Effective Index	Group Index	Confinement Factor	Eg(eV)
0.20	3.50603+0.0180649i	4.39128	0.0547857	1.6734
0.22	3.50814+0.0179748i	4.33454	0.0560201	1.69834
0.24	3.50604+0.0179488i	4.29157	0.0571113	1.72328
0.26	3.50559+0.0178834i	4.24697	0.0581804	1.74822
0.28	3.511+0.017806i	4.20386	0.0574174	1.77316
0.30	3.5038+0.0178269i	4.17422	0.0606124	1.7981
0.32	3.49572+0.0178339i	4.15128	0.0620778	1.82304
0.34	3.50381+0.0178269i	4.17422	0.0606124	1.84798
0.36	3.47976+0.0178243i	4.1112	0.0650925	1.87292
0.38	3.47188+0.0178159i	4.09252	0.0664478	1.89786
0.40	3.46171+0.0177474i	4.4178	0.0641069	1.9228

Table 4.4: Effective Index, Group Index, Confinement Factor and Bandgap Energy corresponding to various mole fractions with 2 QW for well width=9.4nm

Mole Fraction(x)	Effective Index	Group Index	Confinement Factor	Eg(eV)
0.12	3.50586+0.0183473i	4.71945	0.0405821	1.57364
0.14	3.50694+0.0183588i	4.61434	0.0457795	1.59858
0.16	3.50638+0.0182209i	4.52756	0.0488062	1.62352
0.18	3.50661+0.0180826i	4.45298	0.0.0507468	1.64846
0.20	3.5067+0.0179766i	4.389848	0.0519957	1.6734
0.22	3.50696+0.01789i	4.33506	0.0529334	1.69834
0.24	3.51151+0.01346i	4.41536	0.0.109047	1.72328
0.26	3.5057+0.01780i	4.2479	0.0534362	1.74822
0.28	3.50656+0.01775i	4.2069	0.0540271	1.77316
0.30	3.50337+0.01772i	4.17482	0.056875	1.7981
0.32	3.49525+0.01771i	4.15229	0.0580626	1.82304
0.34	3.48721+0.01770i	4.13105	0.0591515	1.84798
0.36	3.47924+0.01768i	4.11075	0.0601231	1.87292
0.38	3.47134+0.01767i	4.0914	0.0610139	1.89786
0.40	3.46349+0.01767i	4.07301	0.0618631	1.9228

Table 4.5: Effective Index, Group Index, Confinement Factor and Bandgap Energy corresponding to various mole fractions with 1 QW for well width=15nm

Mole Fraction(x)	Effective Index	Group Index	Confinement Factor	Eg(eV)
0.10	3.50478+0.01811i	4.17778	0.0690759	1.5487
0.12	3.50223+0.01858i	4.72412	0.045779	1.57364
0.14	3.50664+0.01860i	4.6018	0.0482684	1.59858
0.16	3.50553+0.01856i	4.52592	0.0564155	1.62352
0.18	3.50667+0.01845i	4.45194	0.0603962	1.64846
0.20	3.5078+0.01837i	4.38907	0.0624965	1.6734
0.24	3.50533+0.01824i	4.29648	0.0639361	1.72328
0.26	3.50492+0.01818i	4.25224	0.0534362	1.74822
0.28	3.50714+0.01813i	4.21072	0.0673679	1.77316
0.30	3.50478+0.01810i	4.1778	0.0690759	1.7981
0.32	3.49719+0.01824i	4.41605	0.0759108	1.82304
0.34	3.4893+0.01826i	4.41653	0.0784331	1.84798
0.36	3.48148+0.01828i	6.08806	0.0809329	1.87292
0.38	3.47373+0.01830i	4.41738	0.0833522	1.89786
0.40	3.46604+0.01832i	4.07992	0.0857023	1.9228

Table 4.6: Effective Index, Group Index, Confinement Factor and Bandgap Energy corresponding to various mole fractions with 2 QW for well width=15nm

Mole Fraction(x)	Well Width(nm)	QW	Effective Index	Group Index	Conf Fac
0.30	10	1	3.5028+0.0176i	4.1742	0.054958
0.30	10	2	3.5039+0.0178i	4.17447	0.061360
0.32	10	1	3.50287+0.01762i	4.1742	0.054989
0.32	10	2	3.4958+0.0178i	4.15146	0.062897
0.36	10	2	3.4799+0.01786i	4.1114	0.066095
0.30	12	1	3.5030+0.01765i	4.17444	0.0517368

Table 4.7: Effective Index, Group Index and Confinement Factor corresponding to various combinations

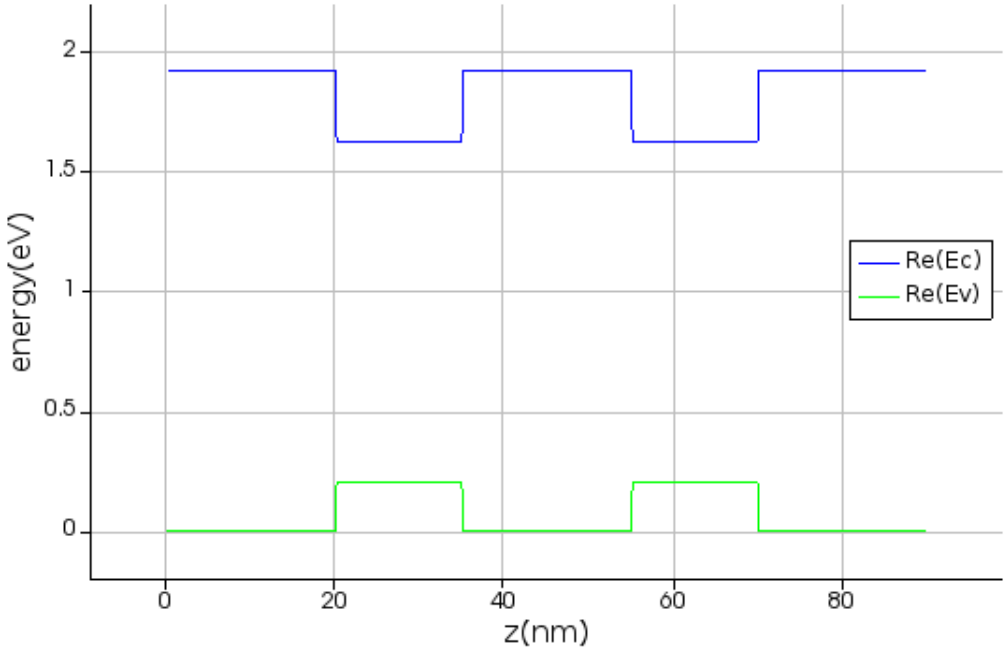

Figure 4.1: Band diagram of the MQW without electric field

4.1.2 Effect of Electric Field on Absorption Spectrum

The Figure 4.3 and Figure 4.4 shows the absorption spectra of $Al_xGa_{1-x}As/GaAs$ without and with the applied electric field. Before the application of an external electric field the absorption spectra is having a higher value. With the application of the electric field the absorption coefficient value is seen to be reduced and also a slight shift in wavelength also occurs. This shows the QCSE.

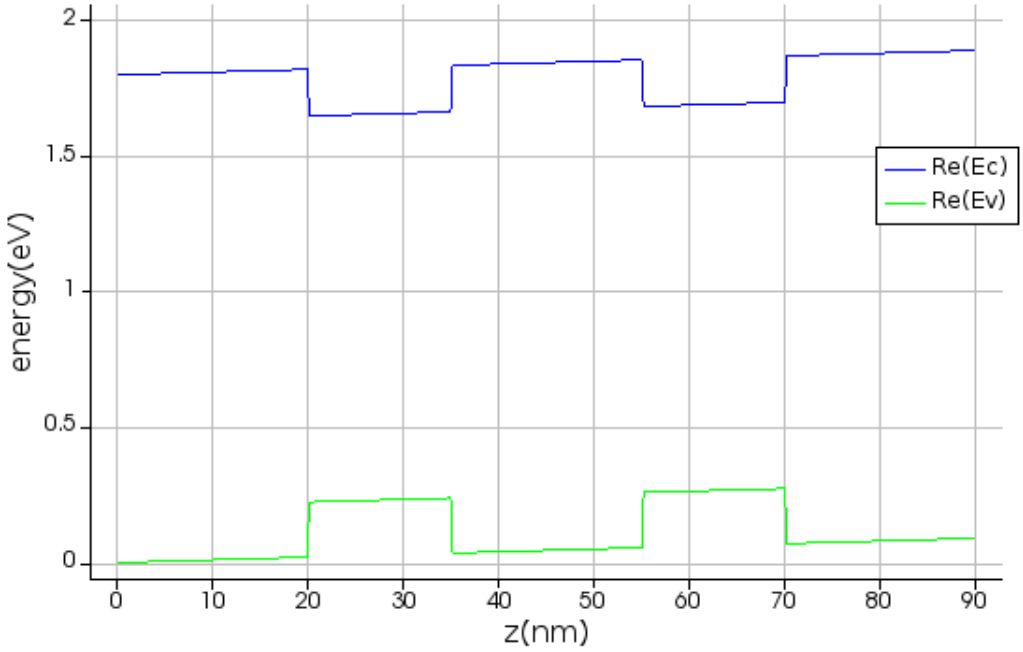

Figure 4.2: Band diagram of the MQW with electric field

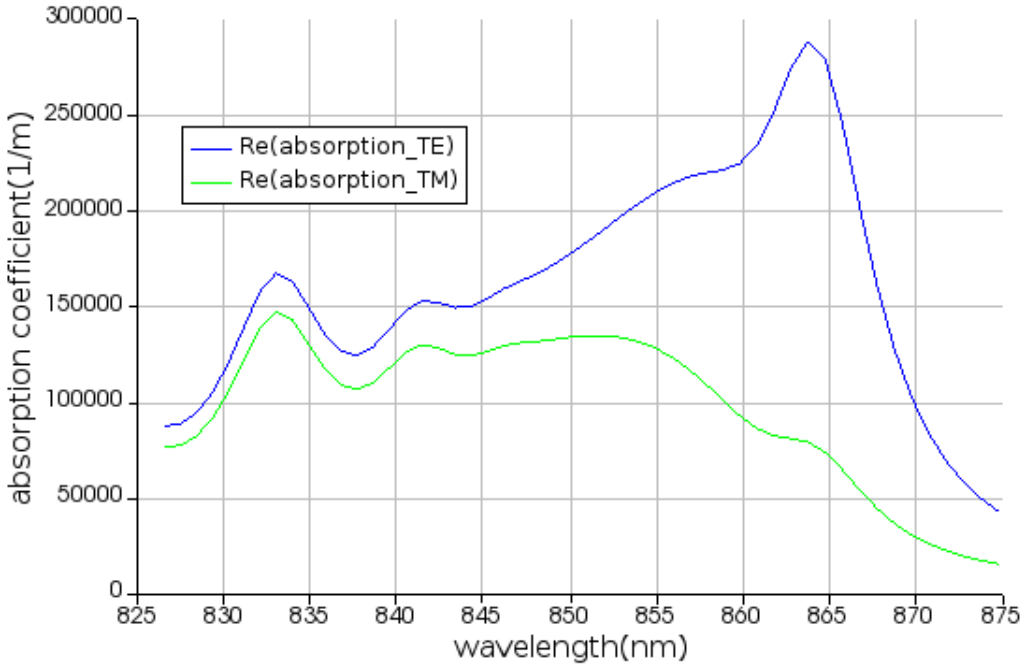

Figure 4.3: Absorption Coefficient without electric field

4.1.3 Effect of Electric Field on Wave Function

The Figure 4.5 shows the wave functions of valance band(holes) and conduction band(electrons) without electric field. When an electric field is applied, electron wave

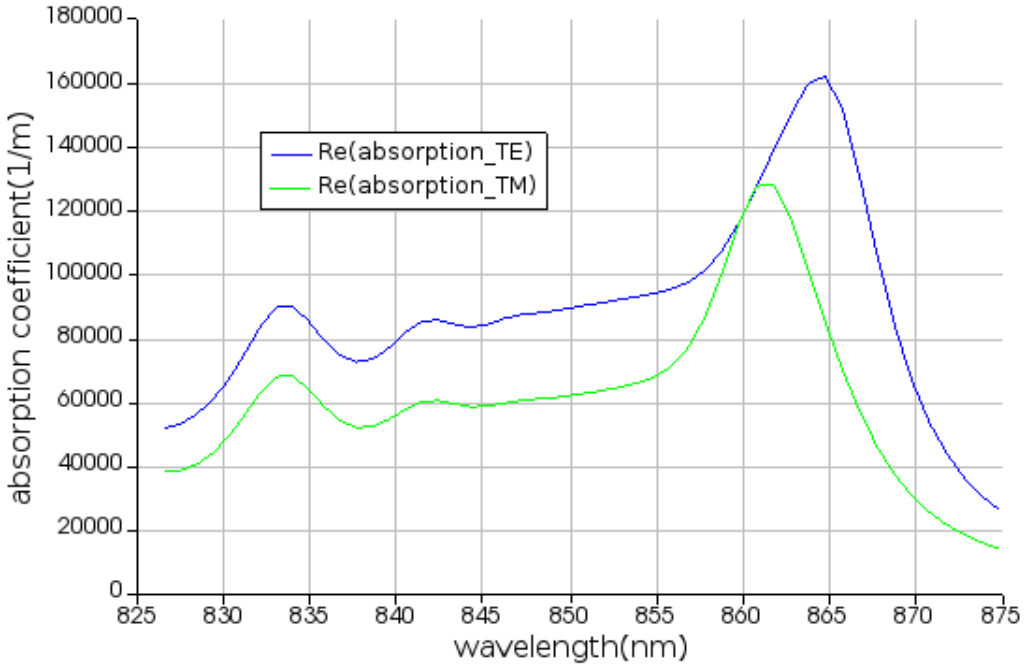

Figure 4.4: Absorption Coefficient with electric field

function shifts towards right and the hole function shifts towards left side. It is shown in Figure 4.6. As we increase the field, this shifting will also increase.

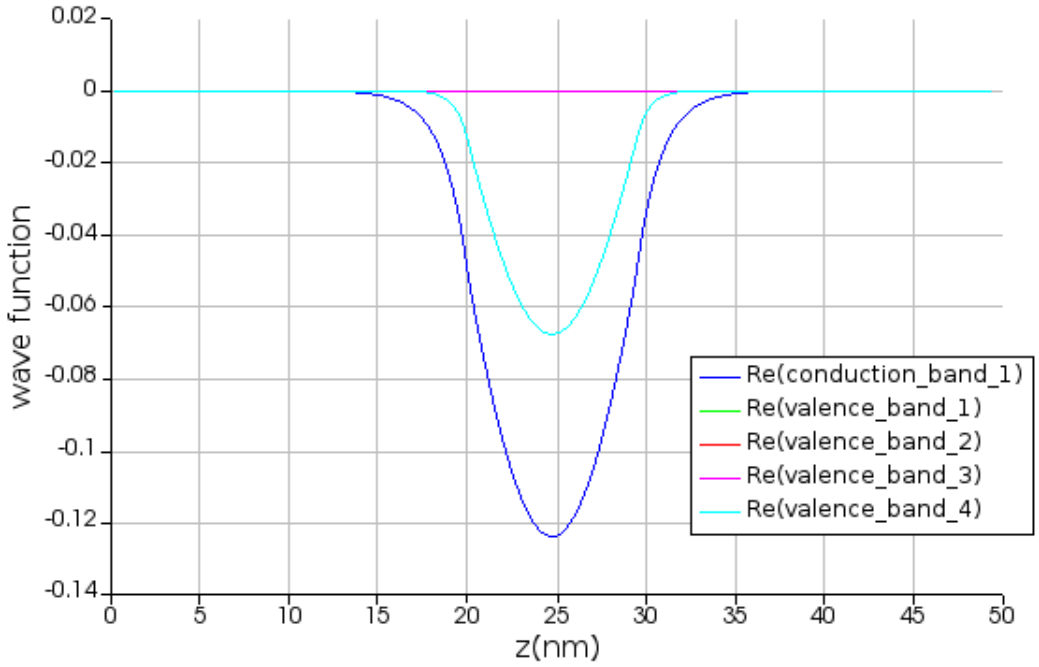

Figure 4.5: Wave function of electron and hole without electric field

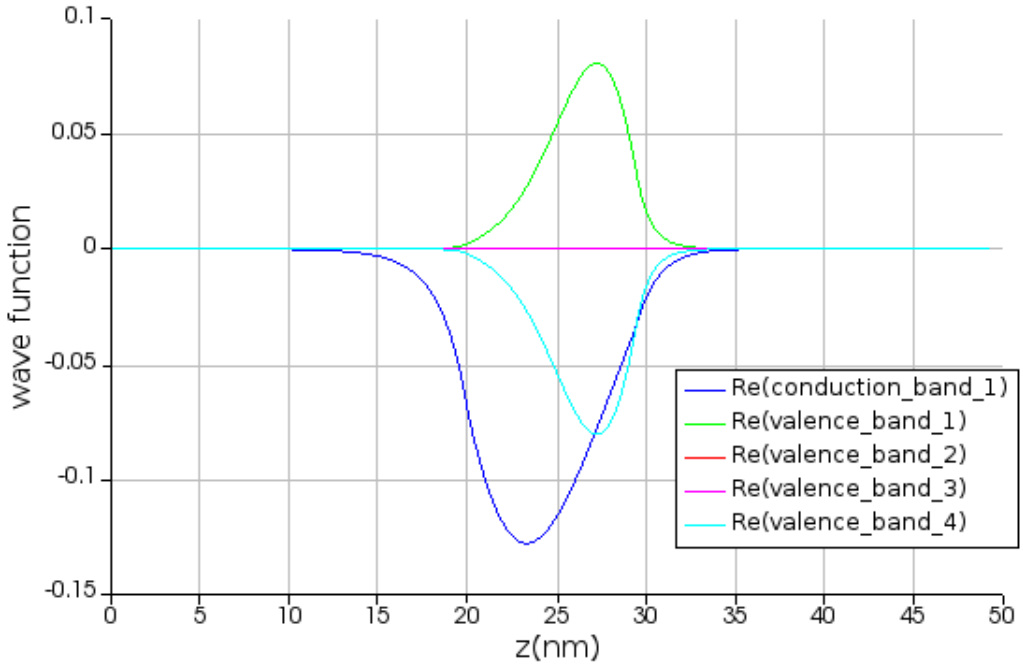

Figure 4.6: Wave function of electron and hole with electric field

4.2 Analysis on the basis of different Electric Fields

The electric field parameter is changed in MQW solver and the absorption coefficient is analysed.

Without the applied electric field, the absorption coefficient was maximum. After the application of electric field the absorption coefficient has varied to a smaller value and a red shift in wavelength is analysed. As we increase the strength of the electric field the absorption coefficient goes on decreasing.

Among that the mole fraction of aluminium with x=0.40, well width=15nm with two QW shown the highest absorption coefficient of $2881.88m^{-1}$. The $\Delta\alpha$ of x=0.40 with two QW is shown in Figure 4.8. $\Delta\alpha$ is change in maximum achievable change in absorption coefficient. The $\Delta\alpha$ of EAM with mole fraction 0.40 and double QW is observed to have a higher value with just the application of 10KV/cm of electric field.

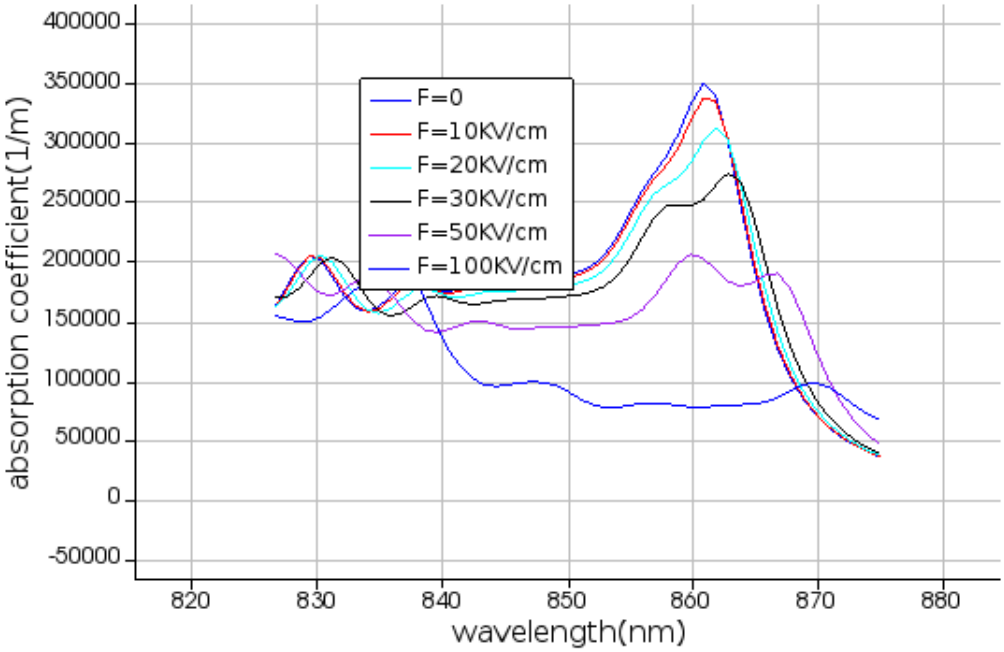

Figure 4.7: Electric Field vs Absorption Coefficient

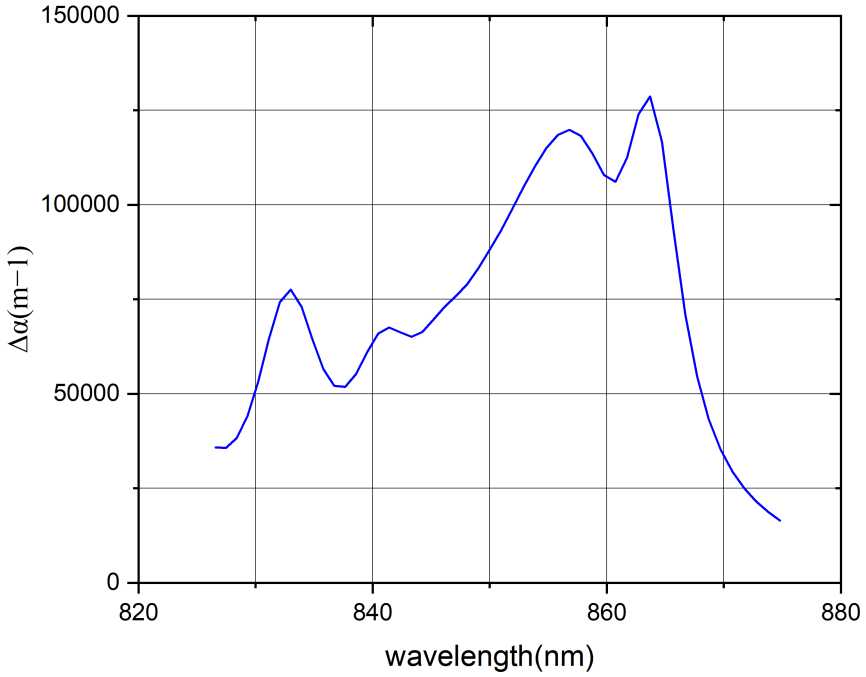

Figure 4.8: $\Delta\alpha$:Change in Absorption Coefficient

4.3 Operating Wavelength(λ_{op})

The wavelength corresponding to lowest value of absorption coefficient without applied field and on the same wavelength the absorption coefficient increases as the electric field is applied. The operating wavelength is found to be 874.803nm. The operating wavelength can be analysed from the absorption coefficient versus wavelength graph given on Figure 4.7.

4.4 Insertion Loss and Extinction Ratio

Among the combinations simulated, the combination with mole fraction of 0.30, well width of 12nm and one quantum well was found to have a minimum insertion loss and maximum $\Delta\alpha/\Delta F$ is observed. Insertion loss is analysed as 0.4477dB and an extinction ratio of 4.764dB.

Chapter 5

Conclusion and Future Scope

In this work, we examined a $Al_xGa_{1-x}As$/GaAs EAM of different mole fractions of $Al_xGa_{1-x}As$ with one and two QW with and without field and varying well width separately. Analysis of the band diagram, absorption spectra, and wave function is also done. It proves the QCSE very vividly. Large absorption shifts at low fields can be obtained by using numerous QWs.

As we increase the electric field the absorption coefficient is found to diminish to lower values and in the case of wavelength a red shift is observed. As the number of QW is increased a significant increase in absorption coefficient is noticed. A high value of $\Delta\alpha$ is desired. For this purpose growing more QW is desirable. But it leads to an increase in the required voltage.

The insertion loss of various combinations is analyzed. The insertion loss should be minimum and $\Delta\alpha/\Delta F$ should be maximum for the application of EAM in optical communication. The combination with mole fraction 0.30, well width of 12nm with one QW was found to have the minimum insertion loss of 0.4477dB. An extinction ratio of 4.764dB is found for this combination.

In future this simulation can be done considering the temperature dependence also. It can be employed in switching applications due to it's faster switching rate. This study can be made use in ring resonators due to it's better absorption performance.

References

[1] T. H. Wood, "Multiple quantum well (MQW) waveguide modulators", in Journal of Lightwave Technology, vol. 6, no. 6, pp. 743-757, June 1988, DOI: 10.1109/50.4063.

[2] M. E. Chin and W. S. C. Chang, "Theoretical design optimization of multiple quantum well electroabsorption waveguide modulators", in IEEE Journal of Quantum Electronics, vol. 29, no. 9, pp. 2476-2488, Sept. 1993, DOI: 10.1109/3.247705.

[3] S. Panda et al., "Quantum Confined Stark Effect And Optical Absorption in $Al_xGa_{1-x}As$ $/GaAs/Al_xGa_{1-x}As$ Single Quantum Well", DOI:org/10.1002/pssb.2221940212.

[4] P.L.Souza et al., "Amplitude modulators based on the stark effect", in Elsevier Microelectronics Journal, 2002, DOI: 10.1016/S0026-2692(01)00129-X.

[5] T. Hiraki et al., "50-GHz-Bandwidth Membrane InGaAsP Electro-Absorption Modulator on Si Platform," in Journal of Lightwave Technology, vol. 39, no. 16, pp. 5300- 5306, 15 Aug.15, 2021, DOI: 10.1109/JLT.2021.3082710.

[6] R. Dingle, Wiegmann, et.al., "Quantum States of Confined Carriers in Very Thin $Al_xGa_{1-x}As/GaAs/Al_xGa_{1-x}As$ Heterostructures". Physical Review Letters, 33(14), 827–830, 1984. DOI:10.1103/physrevlett.33.827.

[7] Wight et.al., "Limits of electro-absorption in high purity GaAs, and the optimisation of waveguide devices", in IEE Proceedings J Optoelectronics, 135(1), 1988. DOI:10.1049/ip-j.1988.0010.

[8] L. Ji et al., "Design of an Electro-Absorption Modulator Based on Graphene-on-Silicon Slot Waveguide," in IEEE Photonics Journal, vol. 11, no. 3, pp. 1-11, June 2019, Art no. 7800911, DOI: 10.1109/JPHOT.2019.2918314.

[9] Chao and Chuang, "Momentum-space solution of exciton excited states and heavy-hole-light-hole mixing in quantum wells", in Physical review. B, Condensed matter, 48 11, 8210-8221, 1993.

[10] L. Vina, R. T. Collins, E. E. Mendez and W. I. Wang, "The Evolution of Quantum Structures", in Phys. Rev. Lett. 58,832, 1987.

[11] P.J Mares and S. L Chuang, "Modeling of self-electro-optic-effect devices", in Journal of Applied Physics, vol.74, no.2, 1388–1397, July 1993, DOI:10.1063/1.354897.

[12] Hung Sik Cho and Paul R Prucnal, "Effect of Parameter Variations on the performance of $GaAs/Al_xGa_{1-x}As$ Multiple Quantum Well Electroabsorption Modulators", in IEEE Journal of Quantum Electronics, vol.25, no.7, July 1989.